Astron. Astrophys. 354, 621–635 (2000)

ASTRONOMY AND ASTROPHYSICS

T Tauri stars: The UV/X-ray connection

V.M. Costa[1,2], **M.T.V.T. Lago**[1,3], **L. Norci**[4], **and E.J.A. Meurs**[4]

[1] Centro de Astrofisica da Universidade do Porto, Rua das Estrelas, 4150 Porto, Portugal
[2] Departamento de Matemática, Instituto Superior de Engenharia do Porto, Portugal
[3] Departamento de Matemática Aplicada, Faculdade de Ciências da Universidade do Porto, Portugal
[4] Dunsink Observatory, Castleknock, Dublin 15, Ireland

Received 26 March 1999 / Accepted 22 November 1999

Abstract. We have analysed newly calibrated IUE and ROSAT data for three T Tauri stars from different subclasses: TW Hya, V410 Tau and CS Cha, a Classical T Tauri star (CTTS), a Weak T Tauri star (WTTS) and a T Tauri star intermediate between CTTS and WTTS, respectively. In the ultraviolet the continuum seems to be well explained by the sum of the stellar black body emission plus a hydrogenic component with temperature in the range 1.4 to 5×10^4 K. TW Hya requires additionally a third component at 7900 K covering approximately 5% of the stellar surface. Using UV line fluxes, we have also analysed the energy emitted by these stars up to temperatures of 10^5 K. All three stars show emission strongly enhanced relatively to the Sun and peaking at temperatures characteristic of the transition region. In this respect the behaviour of the three stars seems to extend in a harmonic way from the ultraviolet into the X-ray band. The X-ray spectral analyses are consistent with emission from a two-temperature, optically thin plasma in collisional equilibrium. The lowest temperature plasma is at about 10^6 K while the highest reaches 10^7 K. We have also checked for and found no evidence for flaring activity in our sources at the time of the observations. Nevertheless, some level of variability is present for the stars in the sample. The ROSAT datasets for V410 Tau show a variation in terms of count rate on timescales of months to years.

Key words: stars: evolution – stars: pre-main sequence – ultraviolet: stars – X-rays: stars

1. Introduction

T Tauri stars (TTS) are young ($\leq 10^7$ years) low mass ($< 3\,M_\odot$) stars still contracting towards the Main Sequence. They show an absorption spectrum characteristic of late F to M, yet in many cases overlapped by emission lines of H, Mg II and Ca II, amongst others. Based on the strength of the Hα equivalent width some authors classify the TTS in two sub-classes: Classical TTS (W(Hα)>10 Å) and Weak TTS (W(Hα)<10 Å). Compared to other stars of similar effective temperature most TTS exhibit a significant excess continuum radiation in the ultraviolet, optical and infrared.

Send offprint requests to: vcosta@astro.up.pt

T Tauri stars have been widely observed at multiwavelength bands. This has been prompted by the broad interest raised by the challenging properties of these stars as well as by their importance as analogues to the Sun in its very early stages of evolution. The ultraviolet is no exception. One of the most relevant results in the ultraviolet for TTS has been the evidence for the presence of emitting regions with temperatures up to 10^5 K, strongly enhanced relatively to the Sun (Gahm et al. 1979; Lago et al. 1984). The UV continuum of TTS has been explained in terms of two components: the long wavelength being dominated by the stellar flux and the short wavelength by free-free and free-bound emission from plasma between 2 and 5 10^4 K (Lago et al. 1984).

Variability both in the continuum and in the lines seems to be a frequent characteristic of these stars. Evidence comes from data at various wavelengths. In the visible for instance, strong variability has been observed in the lines, both in terms of flux or shape of the profiles, and for some stars also in the continuum, although to a much lesser extent. Some stars display quasi-periodic variations, in others the variability is just irregular. The optical periodic variability of some TTS has been interpreted in terms of rotational modulation by large spots (amongst others, Catala & Bertout 1990; Fernández & Miranda 1998). Variability has also been detected in the ultraviolet which in some cases has been atributed to surface spots (namely, Vrba et al. 1986; Fernández & Eiroa 1996). Other authors found explanation in accretion-related activity (see e.g. Castro & Fernández 1996). As for variability, the X-ray spectral region is no exception and it is present for CTTS and WTTS alike (e.g. Montmerle et al. 1983; Casanova et al. 1995). Flare-like activity has also been reported (Gahm et al. 1995; Skinner et al. 1997).

These phenomena have been interpreted in terms of solar-type magnetically driven activity. They seem to result from rapid changes of the level of activity and/or the conditions prevailing in the atmosphere of the stars on time scales of hours to tens of minutes (Lago & Gameiro 1998).

Some authors have associated the observed properties of CTTS with the presence of strong stellar winds (e.g. Penston & Lago 1983; Edwards et al. 1987). Others favour the interpretation of being the result of circumstellar accretion disks, namely invoking mass infall channelled by strong stellar magnetic fields (Uchida & Shibata 1984; Bertout et al. 1988; Königl

1991; Cameron & Campbell 1993). Yet some recent data do not support the dominance of accretion in TTS, for example the analysis of the Hα line profile for a large and consistent sample of TTS (Reipurth et al. 1996).

Observations with the *Einstein Observatory*, ROSAT and ASCA (Walter & Kuhi 1981; Schmitt et al. 1990; Feigelson et al. 1993; Neuhäuser et al. 1995; Carkner et al. 1996, amongst others) show that X-ray emission is also a characteristic of TTS. This emission is found to be variable in many cases and appears consistent with thermal emission from an optically thin, solar-like coronal plasma. Early works dealing with *Einstein* data found evidence for emission from plasma at energies ~ 1 keV (Walter & Kuhi 1981). However with ROSAT data the X-ray spectra of TTS have better been reproduced by means of a two-temperature thermal plasma model (Feigelson et al. 1994; Carkner et al. 1996 and this work). Furthermore, powerful flares, up to 10^{32} erg/sec in a single observation, have been observed in some sources on time scales of minutes to hours (Preibisch et al. 1993; Skinner et al. 1997).

These properties resemble those seen in the Sun and in other magnetically active late-type stars, such as RS CVn binary systems. In these stars the plasma is heated by continuous and/or explosive events and is trapped in closed magnetic structures attached to the star. From the correlation between stellar rotational period and X-ray emission observed in some TTS it has been concluded that a solar-like dynamo mechanism may be responsible for the observed properties (Bouvier 1990; Neuhäuser et al. 1995). However additional energy supply (e.g. MHD waves or accretion of matter) must be present in some TTS because the level of radiative losses in the emission lines is about two orders of magnitude higher than that of magnetically active dwarfs and evolved binaries (Alcalá et al. 1997). Moreover, unpredicted correlations between L_X and the stellar luminosity L_{bol} have been found for several star formation regions (SFR) in contradiction with the solar analogy (e.g. Feigelson & Kriss 1989; Neuhäuser et al. 1995; Wichmann et al. 1997).

In this paper we will address the UV/X-ray connection in TTS. In order to model these stars it is important to clarify the structure of their atmosphere and to compare the amounts of emission in the various temperature regions. The combination of low resolution IUE and ROSAT data addressed in this work is essential for such an analysis.

We present and discuss combined ultraviolet and X-ray data for 3 TTS. Our sample includes a CTTS, a WTTS and a third one which does not quite fit into this classification scheme as so often happens with TTS. In Sect. 2 we summarize the general properties of the stars in our sample. In Sect. 3 we present the line identifications in the UV spectra together with an analysis of the continuum. A detailed X-ray analysis of the sources follows in Sect. 4, where ROSAT spectra are fitted by a two-temperature model and the detected stars are searched for X-ray emission variability. In Sect. 5, we draw a comparison with the Sun. Finally, in Sect. 6 we present the conclusions and discuss the implications of our findings towards understanding the structure of the outer layers of these 3 TTS.

2. The sample of stars

In this section we present a brief overview of the global properties of the three stars considered in this paper.

2.1. TW Hya

TW Hya is one of the closest CTTS, at a distance of 56 pc. It is located in a region devoid of dark and CO clouds. The understanding of such isolated TTS is of special interest. It allows a more direct study of the properties of the stars without the interference of the environmental circumstellar material. Further, scenarios different from those proposed for star formation in large clouds have to be invoked.

TW Hya displays a photospheric absorption spectrum which is consistent with a K7 V type (Herbst & Koret 1988). In the optical the spectrum shows strong emission lines of hydrogen which are highly variable. Emission lines of He I, Ca II, Fe II, and [O I] are also present (Rucinski & Krautter 1983). The Li I line, although not very strong, is in absorption. The Hα line is very intense (≈ 190 Å equivalent width) and broad. The profile is approximately triangular in shape, with a small blue displaced absorption, the most common type of Hα line profile amongst TTS (Reipurth et al. 1996). TW Hya is a very active TTS varying on time scales of 1 day to a few hours. In 1983, its photometric variability was observed to be quite erratic. Short time-scale trends of a few hours in duration were seen to be superimposed on, or combined with longer night-to-night variations, with a total range of $10.9 < V < 11.3$ (Rucinski & Krautter 1983). The interesting properties of this star led some authors to analyse its behaviour at X-rays (Kastner et al. 1997; Hoff et al. 1998; Jensen et al. 1998) which we will review in Sect. 4.

2.2. V410 Tau

V410 Tau, a binary star (Ghez et al. 1993) which is likely a close counterpart to the Sun at an age of one million years (Herbst 1989) and located at a distance of 140 pc, is one of the brightest WTTS with V = 10.6-11.2 and $L_{bol} \approx 2.3 L_\odot$ (Joncour et al. 1994). It is also a K7 V star but with weak Hα and H, K of Ca II in emission and strongly absorbed Li I (Herbig & Bell 1988). However, its spectral type has been quoted as K2-K4 in different works (Basri & Batalha 1990; Bouvier et al. 1986).

This star has been extensively observed at all wavelength bands, from radio to X-rays. The light curve of V410 Tau exhibits strong variations in amplitude and shape, up to 0.6 mag at V. The period is always found to be 1.87 days and the variations have been interpreted as rotational modulation by large surface spots (Bouvier et al. 1989; Fernández & Miranda 1998). Petrov et al. (1994) explained the 1986-1992 light curve by means of one large spotted area changing in size and temperature. Recently, the periodic variability was seen to extend to the absorption lines, the continuum and the Hα emission (Fernández & Miranda 1998). Also, they have found variations on time scales of months in the Hα emission. A first analysis of one of the ROSAT observations of V410 Tau was presented by Strom &

Strom (1994). ROSAT all-sky survey data for this star are reported by Neuhäuser et al. (1995).

2.3. CS Cha

The Chamaeleon I cloud has been the most thoroughly investigated of the three dark clouds composing the Chamaeleon star forming region. It is the largest of the three and apparently the oldest, with an estimated age of 2-3 Myrs (Gauvin & Strom 1992). One difficulty concerning Chamaeleon I is the uncertainty in its distance, with published estimates from 115 to 212 pc. However, the value now widely accepted is 140 pc (Schwartz 1992). CS Cha is a not widely studied K5 V TTS, with several properties of a CTTS. However, its near-infrared spectral energy distribution is different from that found for CTTS, in the sense that this star shows no substantial excess emission in this spectral range. The Hα line profile is very similar to the one of TW Hya (Reipurth et al. 1996). Being member of the Chamaeleon association the mass of CS Cha is estimated to be 0.9 - 1.2 $M_\odot$ and L_{bol} = 1.32 $L_\odot$ (Lawson et al. 1996). This star is included in the sample of TTS studied with ROSAT by Alcalá et al. (1995) and Preibisch (1997).

3. The UV observations and analysis

We have used low dispersion calibrated spectra selected from the IUE Newly Extracted Spectra (INES) with a limiting resolution in the range 6-7 Å. For each star the date, camera, image number and exposure time of each spectrum are given in Table 1. Whenever possible we include more than one spectrum per star, which have been added to improve the S/N. The individual signal-to-noise ratios (S/N) are shown in Table 1. However, they are merely indicative and were obtained at ≈ 1700Å and ≈ 3000Å for SW and LW spectra, respectively. After adding the available spectra we obtained for V410 Tau a S/N = 3 for the SW and S/N = 9 for the LW. We should point the fact that the S/N is strongly wavelength dependent. For the analysis of the spectra we have used the FIGARO package.

3.1. The line identification

We have identified the emission lines present in the UV spectra of the TTS in the sample: TW Hya, V410 Tau and CS Cha. As seen in Fig. 1 through 3, these stars show a different behaviour in terms of their UV emission that we will analyse in detail.

While TW Hya (Fig. 1) shows strong emission lines (corresponding to excitation temperatures up to $2\,10^5$ K), the lines displayed by V410 Tau (Fig. 2) and CS Cha (Fig. 3) are relatively weak and only a few can be reliably identified. Especially, in the case of CS Cha since the spectra are quite noisy. For each star Table 2 gives, for each of the lines identified, the corresponding peak emission temperature, the observed flux and associated uncertainties, the computed flux at the star's surface and the ratio of this flux to the flux emitted by the Sun in the same line. The errors associated to the measured fluxes may result from observational and statistical uncertainties. The main contributors to the observational errors include the instrumental errors and those associated with the data reduction techniques. In addition, there are errors introduced by the line fitting procedures which are statistical in nature.

Table 1. Log of IUE data. Also shown are the S/N (see text for details).

Object	Date	Camera and Image Number	T_{exp} (min.)	S/N
TW Hya	1979 Oct 29	SWP 7036	152	10
	1979 Oct 29	LWP 5966	60	10
	1984 Jul 16	SWP 23471	100	4
V410 Tau	1979 Oct 29	SWP 7035	180	2
	1993 Oct 2	SWP 48829	325	2
	1989 Jan 21	LWP 14882	45	6
	1989 Jan 21	LWP 14891	45	5
CS Cha	1985 Jan 13	SWP 24900	340	2
	1987 Oct 87	LWP 11880	200	10

As indicated in Table 2, the Si III multiplet ($\lambda \sim 1301$Å) is blended with the OI multiplet ($\lambda \sim 1303.5$Å) and it is difficult to separate the two contributions. However, Si III seem to be the main contributor ($\sim$ 70% of the flux, see Brooks et al. (1999) for a detailed discussion) and we have therefore identified the line as Si III in Figs. 1 and 3. The Fe II lines have been identified for wavelengths between $\sim$2300 and $\sim$2700Å but not measured since they include large blends, mainly of multiplets (1), (2), (3), (32), (35), (36), (47) and (63), amongst others.

As Table 2 indicates the He II line, in the case of CS Cha, is as strong as the C IV line which is not always the case in TTS. This shift of the peak emission to lower temperatures may indicate a higher density atmosphere. In fact, in a collisional-radiative model the ionisation balance is very sensitive to reduced dielectronic recombination at higher densities ($N_e > 7\,10^{11}$ cm^{-3}). See the recent study of the atmospheric structure of the T Tauri star BP Tau using the differential emission measure technique (Brooks et al. 1999). Also see Sect. 5 for further discussion.

As the surface flux is concerned a major source of uncertainty is the value adopted for the radius of the stars, assuming that the distance is well determined. For CS Cha we have followed the work of Lawson et al. (1996) and therefore we assume $R_\star$ = 1.8 $R_\odot$. Whereas, in the case of V410 we followed Petrov et al. (1994) assuming $R_\star$ = 2.6 $R_\odot$ (see also Bouvier 1990). For TW Hya, we are not aware of any published value for the radius of this star. A way of deriving the radius of a star is by making use of the L_{bol} and the T_{eff}. However, some unknown contributions to L_{bol} due to accretion or some other heating mechanism at work in TTS may lead to overestimating the radii and, consequently, underestimating the surface fluxes. Throughout we adopted a value of 1.1 $R_\odot$ for TW Hya.

3.2. The continuum

For TTS the UV continuum is in general well fitted by a two-component model: a black body emission at the star's effective temperature and an optically thin hydrogenic free-free plus free-bound emission usually at a much higher temperature (Lago et

Table 2. Emission lines in the low resolution ultraviolet spectra of the stars TW Hya, V410 Tau and CS Cha obtained with the IUE. T represents the peak emission temperature in Kelvin, f_{obs}, $f_\star$ are the observed and the surface fluxes, respectively and $f_\odot$ the corresponding surface value for the Sun. The flux units are erg $s^{-1}cm^{-2}$. The errors associated to the observed fluxes are denoted as Δf_{obs}. The last column gives the ratio of the stellar to the solar surface fluxes. The flux for the N V line should be taken with caution due to the wing of the strong adjacent Ly α line. For V410 Tau the NV and Si IV flux measurements are only upper limits. Furthermore, the Si II line is slightly displaced relatively to the expected wavelength and is an uncertain identification. The superscript * indicates that the lines are blended.

Object	Line	Wavelength (Å)	T	f_{obs}	Δf_{obs}	$f_\star$	$f_\star/f_\odot$
TW Hya	N V	1238, 1242	2.0×10^5	3.1×10^{-13}	4.8×10^{-14}	2.4×10^6	3313
	O I*, Si III*	1303	$4.7\text{–}5.0\times10^4$	7.3×10^{-13}	2.3×10^{-14}	5.4×10^6	
	C II	1335	2.0×10^4	3.4×10^{-13}	2.2×10^{-14}	2.5×10^6	380
	Si IV	1393, 1402	7.9×10^4	4.9×10^{-13}	7.5×10^{-14}	3.5×10^6	1003
	C IV	1548,1551	1.1×10^5	1.1×10^{-12}	3.7×10^{-14}	7.8×10^6	1240
	He II	1640	1.0×10^4	5.8×10^{-13}	2.9×10^{-14}	4.2×10^6	3124
	Si II	1808,1817	1.5×10^4	1.7×10^{-13}	9.0×10^{-15}	1.2×10^6	50
	Mg II	2795, 2802	8.9×10^3	4.0×10^{-12}	1.4×10^{-14}	2.6×10^7	23
CS Cha	N V	1238, 1242	2.0×10^5	6.5×10^{-14}	1.8×10^{-14}	1.6×10^6	2195
	C IV	1548,1551	1.1×10^5	1.4×10^{-13}	1.8×10^{-14}	3.1×10^6	486
	He II	1640	1.0×10^4	1.1×10^{-13}	9.2×10^{-15}	2.3×10^6	1766
	Mg II	2795, 2802	8.9×10^3	3.2×10^{-13}	1.5×10^{-14}	6.0×10^6	5
V410 Tau	N V	1238, 1242	2.0×10^5	$<5.5\times10^{-15}$	3.0×10^{-15}	$<4.8\times10^4$	<67
	O I*, Si III*	1303	$4.7\text{–}5.0\times10^4$	1.3×10^{-14}	1.8×10^{-15}	1.2×10^5	
	Si IV	1393, 1402	7.9×10^4	$<1.7\times10^{-14}$	$2.\times10^{-14}$	$<1.4\times10^5$	<40
	C IV	1548, 1551	1.1×10^5	4.4×10^{-14}	8.7×10^{-15}	3.6×10^5	57
	He II	1640	1.0×10^4	3.7×10^{-14}	5.5×10^{-15}	3.0×10^5	231
	Si II	1808, 1817	1.5×10^4	2.9×10^{-14}	4.6×10^{-15}	2.3×10^5	10
	Mg II	2795, 2802	8.9×10^3	2.9×10^{-13}	1.0×10^{-14}	2.1×10^6	2

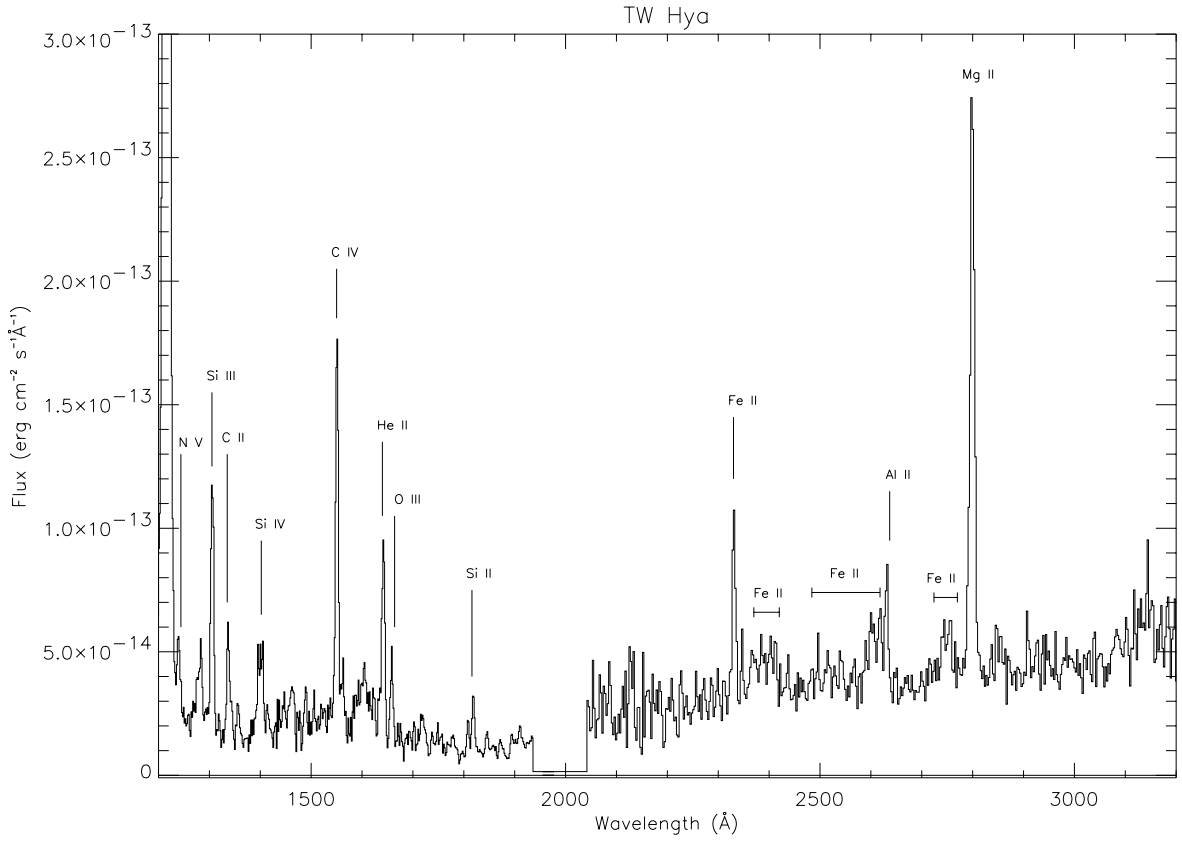

Fig. 1. IUE low dispersion spectrum for the star TW Hya where the main lines have been identified. The spectrum is strictly a merge of two added short and one long wavelength spectra. The region around 2000 Å has been suppressed due to the very high level of noise.

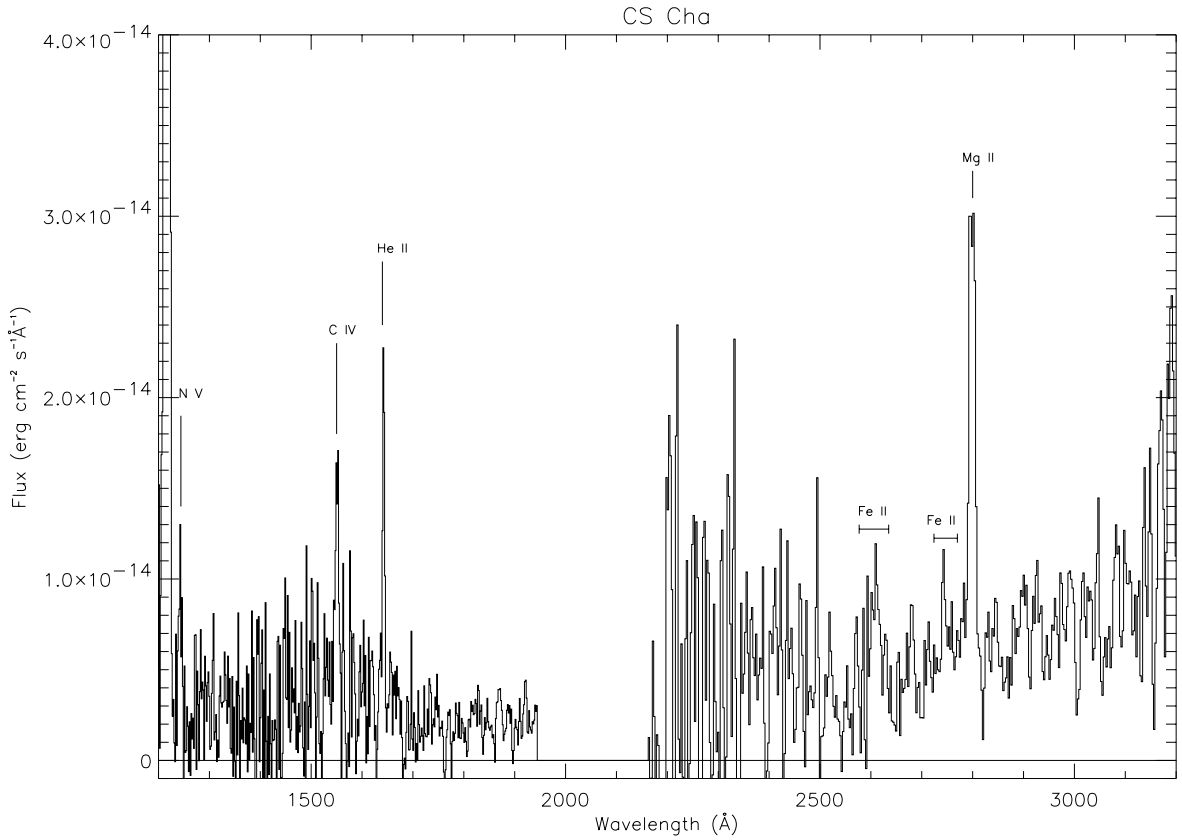

Fig. 2. IUE low dispersion spectrum for the star CS Cha where the main lines have been identified. The spectra are much noisier than in Fig. 1, yet it is still possible to identify the main lines and measure the respective flux.

Table 3. Windows used for fitting the ultraviolet continuum.

Nr.	Wavelength range (Å)
1	1243 - 1275
2	1368 - 1379
3	1680 - 1720
4	2285 - 2305
5	2640 - 2660
6	3037 - 3100

al. 1984). We have done a similar analysis for the stars in the present sample.

For each of the combined spectra we have defined several continuum windows (listed in Table 3 and also shown in Fig. 4) as free as possible from spectral features. The wavelength ranges given in Table 3 should be taken as indicative. Depending on the quality of the spectra, there are cases where one or more windows were narrowed or even dropped. We have used these windows to adjust a black-body spectrum at the star's effective temperature plus the sum of hydrogenic free-free plus free-bound spectra. The temperatures which fit best those windows were obtained using the "Lavenberg-Marquard least squares method" (Press et al. 1986). Another parameter determining the quality of the fit is A_V. Whenever possible we have used the value of A_V given in the literature or otherwise calculated using the distances quoted in Sect. 2 adopting a "mean" interstellar extinction law (Savage & Mathis 1979). The value of A_V producing the best fit is then compared with the initial value (see Sect. 4.2 for the discussion). The success of such fits is difficult to assess for several reasons. Probably the most important is that the selected continuum windows may still have some residual contamination from lines which are unresolved at the dispersion of the spectra used.

For the star TW Hya the best fit was found to correspond to a stellar 4000 K black body emission together with hydrogenic free-free plus free-bound emission at a temperature in the range 3 - 4 10^4 K. Besides these components, the fitting to the longer wavelength region further requires an additional component. The best solution includes also black body emission at 7900 K covering approximately 5% of the stellar surface (Fig. 4). After all, TW Hya is known to be a very active TTS. This is not too different from the recent results for other very active TTS, LkHα 264. In this star the extra component, at T $\sim$ 8700 K covering approximately 4% of the stellar surface, required by the fitting of the UV (long wavelength band) continuum is seen to extend nicely into the optical up to 7000 Å. In both cases accretion would be an explanation. However, magnetic activity at a much higher level than in the Sun is a more atractive alternative in face of other diagnostic tools (Costa et al. 1999). The nature of these two components (the free-free and free-bound emission and the non-stellar blackbody emission) is currently being analysed in terms of their time behaviour in comparison with that of other activity diagnostic tools.

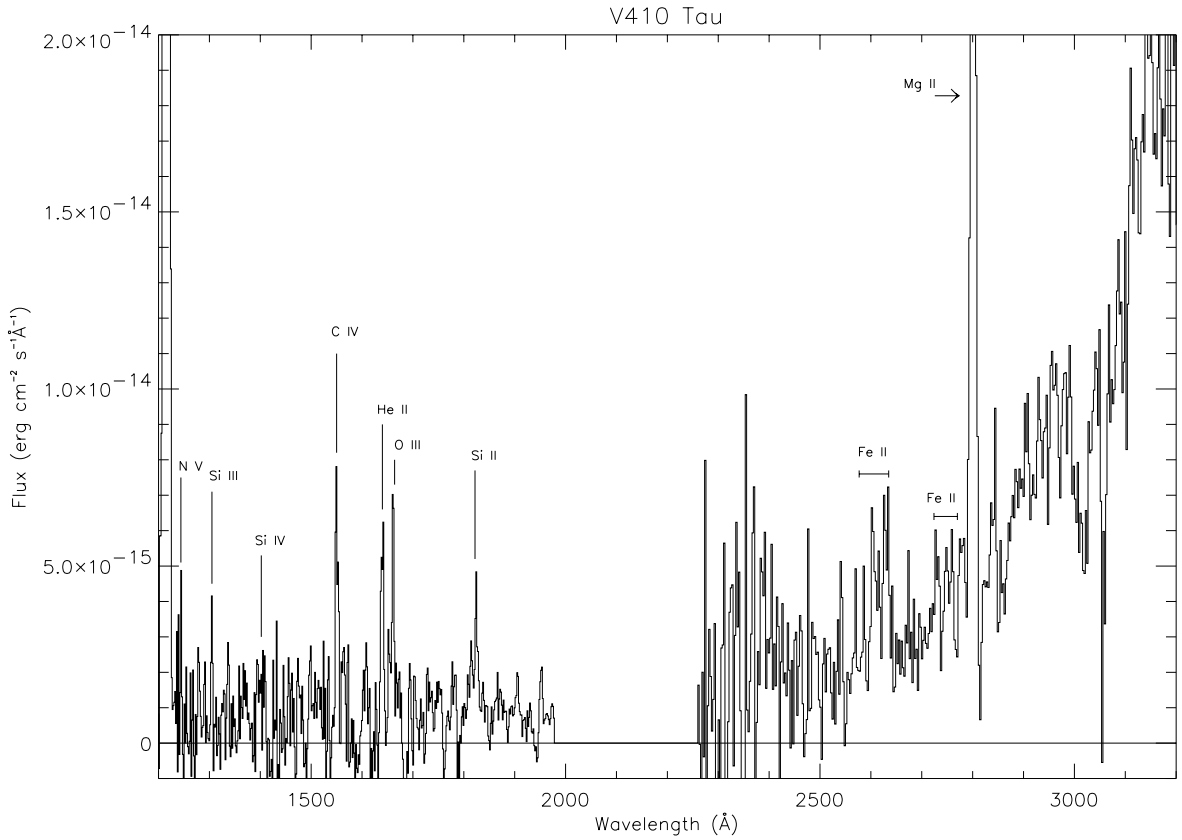

Fig. 3. As in Fig. 2 for V410 Tau.

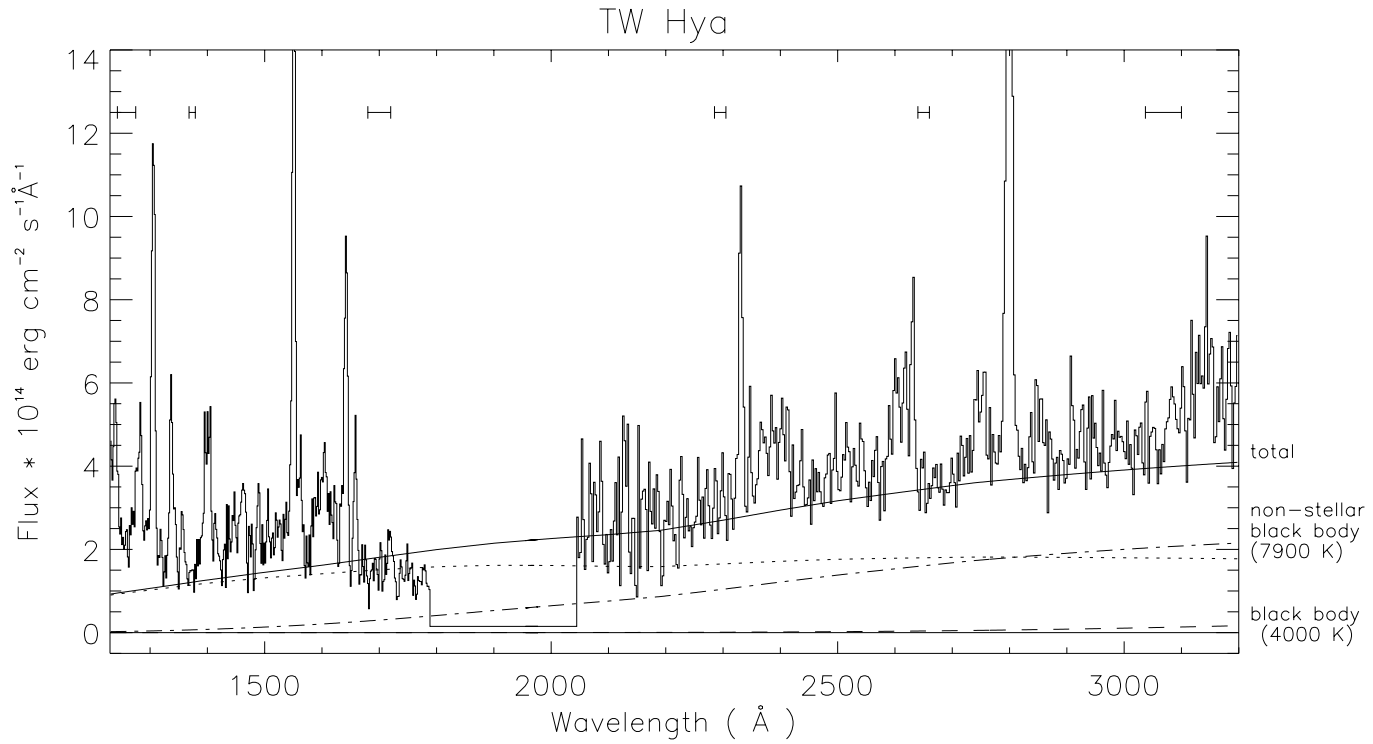

Fig. 4. The best fit to the continuum is the sum of hydrogenic free-free plus free-bound emission (dotted line) at $3\,10^4$ K plus a 4000 K black body emission and a third component - a black body emission at 7900 K covering approximately 5% of the stellar surface. The windows used to fit the continuum are shown (see Table 3). The region around 2000 Å has been suppressed due to the very high level of noise.

The analysis of the continuum was more difficult in the case of V410 Tau and CS Cha because the short-wavelength spectra are noisier. However, we can still derive for the hydrogenic component a temperature in the range 1.4 to 5 10^4 K. For V410 Tau we were able to derive from the longer wavelength band black body emission at a temperature well in agreement with the stellar effective temperature, 4000 K, corresponding to a K7 spectral type as found in the literature from the optical observations. For CS Cha the derived black body temperature is 4300 K, also in good agreement with the spectral type derived from its photospheric spectrum. The conversion of the spectral type to effective temperatures followed the work of Cohen & Kuhi (1979) and Bessel & Brett (1988). However, as stressed in the early work of Cohen & Kuhi, it is not clear what T_{eff} means in a TTS with extended atmospheres, circumstellar dust and, in many cases, circumstellar disks. Therefore, this conversion should be taken with caution. For CS Cha the A_V derived from the fitting of the UV continuum is $\simeq$ 0.25, rather smaller than the value 0.85 given in the literature (Gauvin & Strom 1992). We derived for V410 Tau a value for A_V of 0.10 - 0.2, slightly higher than those found in the literature, A_V = 0.0 - 0.10 (Strom & Strom 1994; Petrov et al. 1994). A much higher value of 0.66 is quoted by Beckwith et al. (1990) which is however inconsistent with the X-ray data (see Sect. 4.2). For TW Hya the value found for A_V is in the range 0.10 - 0.25, still consistent with a small interstellar foreground extinction characteristic of a nearly dust-free region.

4. The X-ray analysis

We have used pointed observations retrieved from the ROSAT Public Data Archive to study the X-ray emission from the stars of our sample. We have analysed spectral shapes as well as variability.

A description of the satellite, the telescope and the detector are given in Trümper (1983) and Pfeffermann et al. (1986).

Table 4 gives the Log of observations.

The data analysis was performed using the Extended Scientific Analysis System (EXSAS) (Zimmermann et al. 1997).

4.1. Source detection and identification

We have applied the source detection program provided in the EXSAS package to all ROSAT observations listed in Table 4. This allows the identification of point-like sources by evaluating an excess of photons above a local and a global background (Cruddace et al. 1988).

In Table 5 we give, besides the name of the object and the observation identification number, the source position as calculated by the detection procedure and the associated errors. The existence maximum likelihood, the offset from the optical position, the off-axis angle (θ), and the count rate are also indicated. The source likelihood of existence (EXI_ML) is defined as EXI_ML = – ln P, where P represents the probability of a spurious detection resulting from a background fluctuation. According with this definition 3,5 and 10 gaussian σ's correspond to a likelihood of existence of 5.9, 14 and 53 respectively.

The table shows that all the stars in our sample are detected with very high probability of existence at positions that appear compatible with their optical counterparts. The accuracy of the source position depends on the distance to the centre of the PSPC detector as the point-spread function (PSF) degrades away from the optical axis. In the central detector region the detection program returns source positions with a precision of a few arcseconds. With a systematic boresight error of the order of 8", a typical working value for the overall positional accuracy is 10" when comparing X-ray and optical positions (Feigelson et al. 1993; Carkner et al. 1996). The optical counterparts of the X-ray sources were checked by inspection of the Guide Star Catalog (GSC). Although some of our X-ray sources have higher offsets values, as the accuracy degrades further off-axis, all the cases outside the central detector area have offsets less than 20" from their optical counterpart as listed in the GSC (which supplies sub-arcsecond positional errors). Since there are no other reasonable alternative optical candidates nearby, we can be very confident about the source identification.

4.2. The spectral analysis

For this kind of analysis we have used the 200065p observation for TW Hya, the 200001p1 observation for V410 Tau and the 200207p observation for CS Cha. These have been chosen because of the long exposure times and the small off-axis angle of the sources of interest. The results of the spectral analysis on the above mentioned frames are summarized in Table 6. The results of the spectral analysis are confirmed by the analysis of the remaining available frames. These observations have been also used to study possible variability (see Sect. 4.3).

We have extracted the source and background photons from the photon event file of each observation. The background was extracted from an annulus concentric with the source extraction circle or, for cases in which other sources are present in the annulus, from regions free of sources as close as possible to the source region. We have selected the pulse height channels between 20 and 235 and binned the spectra in such a way as to obtain the highest possible S/N, as well as enough data points for the fitting program to perform correctly. The corrections for vignetting and dead time have been applied to all datasets.

The usually adopted models for the analysis of ROSAT spectra of TTS are the one or two-component Raymond-Smith models (hereafter, 1T and 2T) which describe the emission from a hot, optically thin plasma in collisional equilibrium (Raymond & Smith 1977).

The parameters in the 1T model are the hydrogen column density, N_H, the plasma temperature, T, and a normalization amplitude, A, in units of cm^{-5}, defined as

$$A = \frac{10^{-14}}{4\pi D^2} EM$$

where D is the distance in cm. From A we can derive the associated emission measure, EM. The free parameters in the 2T model are N_H, the emission measure of both components, EM_1 and EM_2, and the plasma temperatures, T_1 and T_2.

Table 4. Log of the ROSAT data.

Object	Obs. Id.	Obs. Begin	Obs. End	T_{exp} (sec)	Detector
TW Hya	200665p	12 Dec 1991	12 Dec 1991	6712	PSPC
V410 Tau	200001p-0	5 Mar 1991	6 Mar 1991	4486	PSPC
V410 Tau	200001p-1	20 Aug 1991	21 Aug 1991	25591	PSPC
V410 Tau	201312p	8 Sept 1992	11 Sept 1992	2800	PSPC
V410 Tau	201598p	11 Sept 1993	11 Sept 1993	5652	PSPC
V410 Tau	201599p	12 Sept 1993	12 Sept 1993	6175	PSPC
V410 Tau	201600p	13 Sept 1993	13 Sept 1993	5747	PSPC
V410 Tau	201601p	14 Sept 1993	14 Sept 1993	5817	PSPC
V410 Tau	201602p	15 Sept 1993	15 Sept 1993	5582	PSPC
V410 Tau	202156h	13 Feb 1996	13 Feb 1996	7698	HRI
CS Cha	200046p-0	6 Mar 1991	6 Mar 1991	5601	PSPC
CS Cha	200046p-1	26 Feb 1992	27 Feb 1992	3161	PSPC
CS Cha	200207p	18 Feb 1991	24 Feb 1991	31704	PSPC

Table 5. X-ray detections for the three stars.

Object	Ident.	α_{2000}			δ_{2000}			$\Delta\alpha$	$\Delta\delta$	EXI_ML	Offset	θ	counts s^{-1}
		h	m	s	°	′	″	$_s$	″		″	′	
TW Hya	200665p	11	01	52.34	-34	42	22.0	0.3	0.3	9963	5.9	0.25	0.315±0.007
V410 Tau	200001p	04	18	31.11	28	27	19.0	0.5	0.5	4642	2.9	0.28	0.194±0.007
V410 Tau	200001p-1	04	18	31.31	28	27	15.5	0.2	0.3	16619	3.6	0.34	0.214±0.002
V410 Tau	201312p	04	18	30.83	28	27	07.4	0.3	5.0	245	8.7	35.92	0.126 ±0.009
V410 Tau	201598p	04	18	31.63	28	27	35.0	0.3	4.5	554	18.9	40.25	0.123 ±0.006
V410 Tau	201599p	04	18	31.78	28	27	30.0	0.3	4.2	686	13.9	40.33	0.131±0.006
V410 Tau	201600p	04	18	31.44	28	27	34.0	0.4	5.4	297	17.9	40.28	0.098±0.006
V410 Tau	201601p	04	18	31.71	28	27	19.0	0.3	4.5	524	3.0	40.51	0.117 ±0.006
V410 Tau	201602p	04	18	31.33	28	27	28.5	0.3	4.6	513	12.4	40.37	0.123±0.006
V410 Tau	202156h	04	18	30.73	28	27	16.8	0.03	0.3	1592	7.9	12.27	0.075±0.003
CS Cha	200046p	11	02	28.42	-77	33	30.0	1.1	1.1	1680	8.8	16.11	0.072±0.003
CS Cha	200207p	11	02	24.89	-77	33	35.6	0.02	0.3	2304	1.4	11.74	0.079±0.002

Table 6. The best fitting parameters for the spectra using a 2T model, with N_H free and fixed, respectively.

Object	Date of Obs.	Total Counts	S/N	N_H ($10^{20} cm^2$)	kT_1 (keV)	EM_1 ($10^{53} cm^{-3}$)	kT_2 (keV)	EM_2 ($10^{53} cm^{-3}$)	χ^2_{red}
TW Hya	12 Dec 91	2116	9	0.45±0.53	$0.16\pm^{0.07}_{0.09}$	4.46±5.29	$0.86\pm^{0.12}_{0.07}$	2.76±3.00	1.01
				2.66	$0.19\pm^{0.11}_{0.07}$	0.32±0.07	$0.90\pm^{0.07}_{0.05}$	0.26±0.05	0.97
V410 Tau	20 Aug 91	5471	18	2.53±0.51	$0.29\pm^{0.05}_{0.03}$	1.14±0.17	$1.78\pm^{0.30}_{0.14}$	5.65±1.37	1.46
				2.66	$0.25\pm^{0.07}_{0.02}$	1.20±0.13	$1.40\pm^{0.25}_{0.05}$	5.55±0.65	1.41
CS Cha	18 Feb 91	2304	5	7.53±0.86	0.20±0.1	0.67±0.18	$1.16\pm^{0.21}_{0.14}$	1.02±0.17	0.75
				15.1	0.10±0.04	9.14±15.71	$1.04\pm^{0.02}_{0.04}$	1.08±0.37	0.76

We started our analysis by fitting the spectra with a 1T model. In all cases, this model clearly fails to fit the data. Our second approach was therefore to use 2T models. In both cases the spectra are fitted with Raymond-Smith models assuming cosmic abundances and the Morrisson-McCammon interstellar X-ray absorption model (Morrisson & McCammon 1983).

For completeness, we have also tried to fit the data with a power law distribution and a black-body model but they fail to give acceptable reduced-χ^2 values. Taking into consideration the moderate spectral resolution of the PSPC and the S/N of our data, the use of more elaborated models than these four does not seem justified.

Figs. 5 to 7 display the 2T fits for the various spectra as well as the corresponding residuals (lower panel) and χ^2 grids for all spectra (all for N_H fixed - see below).

For each object two fits were performed: one keeping N_H as a free parameter and the other fixing N_H to values taken from the literature. In the first case, a fit with five free parameters to spectral data with ROSAT PSPC resolution may produce quite large fitting errors. This is less a problem in the second case

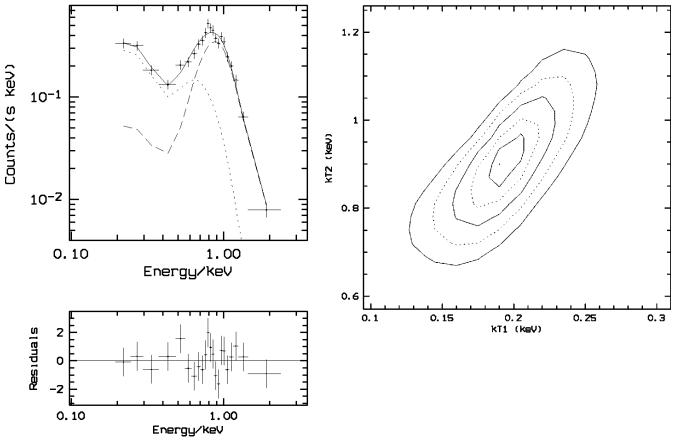

Fig. 5. ROSAT spectrum of TW Hya where the best fitting corresponds to a two-component model. The residuals and a χ^2 grid (68.5%, 90%. 95.5%. 99.73%. 99.99% and 100% confidence contours) are also

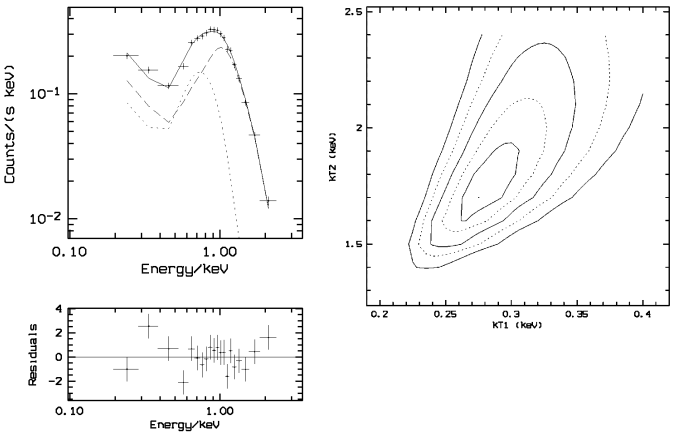

Fig. 6. As in Fig. 5 for V410 Tau.

but the literature values have to be taken with some caution since because of the nature of TTS they are often found embedded in a nebular region which renders N_H determinations not straightforward. Therefore, the hydrogen column density N_H is a critical parameter in the X-ray analysis of TTS. In most cases the A_V values found in the literature have been derived from optical or infrared observations and differences may be found between different authors. We have determined the A_V value for all our objects from the UV observations presented in this work. Some discrepancies occur between the literature values and those obtained in this paper (see Sect. 3.2).

In the case of TW Hya the value of the extinction from optical and/or infrared data is unknown. From the analysis of the Lyman α line in the spectrum of this star, Blondel et al. (1993), suggest a value of A_V = 0.0 mag in order to be consistent with their proposed model for the emission in this line. However, this value has to be taken just as indicative since it is an indirect result and moreover model dependent. The value we obtain in this work through the fitting of the UV continuum is in the range 0.10 - 0.25 mag. This range of A_V translates into a factor of 2 in the uncertainty of the hydrogen density column, showing that

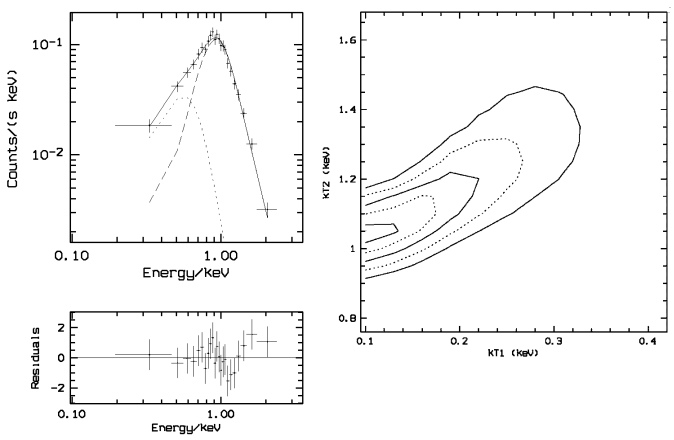

Fig. 7. As in Fig. 5 for CS Cha.

caution should be taken while analysing low count X-ray spectra. In view of the restrictions mentioned regarding the Blondel et al. model approach, we assume, based on our UV results, that some extinction will be present and adopt an intermediate value of A_V = 0.15 for the X-ray spectral modelling.

Optical and IR observations of V410 Tau led to A_V in the range 0.0 - 0.10 (e.g. Strom & Strom 1994; Petrov et al. 1994). Beckwith et al. (1990) give a value for A_V = 0.66. Such a high value of extinction is discarded here on the basis of an extremely poor fit to the X-ray data. We obtained a value A_V = 0.2, for the extinction that, considering the uncertainties, is in agreement with the observations at longer wavelengths. We will therefore adopt A_V = 0.15 as an average of these two independent extinction determinations.

For CS Cha a recent published value of A_V = 0.85 (Gauvin & Strom 1992) is much higher than the value obtained by us of A_V = 0.25 (Sect. 3.2). The difference between these two determinations seems too big to adopt simply some intermediate value for A_V. We employed both these A_V values for the N_H-fixed fits and found that much more reasonable errors for kT_1 and kT_2 result for A_V = 0.85. Therefore this latter value is adopted for the N_H-fixed spectral fit.

We will thus assume in the following A_V = 0.15 for TW Hya, A_V= 0.15 for V410 Tau and A_V = 0.85 for CS Cha in order to calculate the N_H.

We have converted the visual extinction to hydrogen column density N_H using the relation (Paresce 1984).

$$\frac{N_H}{cm^2} = 5.5\,10^{21}\,\frac{E_{B-V}}{mag} = \frac{5.5}{3.1}10^{21}\,\frac{A_V}{mag}$$

In Table 6 we list values of the parameters corresponding to the best fitting 2T model with N_H kept as a free parameter (first row for each star) and with N_H as a fixed parameter (second row), together with the reduced-χ^2 values.

The values obtained for the parameters with the two fitting procedures are often consistent within their errors. Also, with the choices for A_V as described above, the results for N_H from the N_H-free fits are in each case consistent with the adopted values for N_H-fixed. However, a definite improvement on the errors is generally achieved by fitting the data with fixed N_H,

improving most errors by a factor of $\simeq 10$ or more. In the case of V410 Tau our results for the 20 August observation are also in reasonable agreement with those of Strom & Strom (1994). Given the considerable improvement on several of the parameter errors attained with keeping the N_H value fixed, we will discuss in the following only these results.

The values of kT_1 range, considering the errors, between 0.06 and 0.35 keV, indicating the presence of a very soft component of the spectrum in all cases. The harder component has a kT_2 value ranging between 0.79 and 1.94 keV.

TW Hya and CS Cha seem to have more similar values for the two components while in the case of V410 Tau the values of kT_2 are consistently higher than for the other two stars. The X-ray emission from CS Cha has been analysed by Preibisch (1997) under the assumption of a "continuous emission measure model" (CED). He derives a T_{max} around 5.3 keV, which is higher than the temperature for the hottest component obtained with our 2T model fit. However, due to the low number of counts he concludes that it is not possible to discern between the CED and 2T models as to which one fits better the CS Cha spectrum. He also interprets the results using a loop model, but this invokes either loops exceeding several stellar radii in length or too high a pressure, which would require very strong magnetic fields. The presence of such strong fields is not confirmed by observations of TTS. The X-ray luminosity derived from the CED model is higher than the one obtained by us, however given the uncertainties associated with these values, the two values are still consistent (Table 7) showing that both approaches are almost equivalent in this respect. A different value for L_X (1.26×10^{30} erg s^{-1}) has been reported for this star by Feigelson et al. (1993), but this was based on the 1T model.

Based on results from ASCA and EUVE observations some authors claim evidence for an under-abundance of metals in the coronae of some stars relative to the corresponding photospheric values, by a factor between 2 (e.g. Mewe et al. 1996) and 10, in the case of one RS CVn binary (Schmitt et al. 1996). However, using simulations of ASCA/SIS detector spectra and 2T and CED models, Favata et al. (1997) argued that those under-abundances may be just an effect of the fitting procedure. In fact, while fitting the ASCA/SIS, the lower temperature peak around 0.2 keV is not included. The inclusion of the softer band leads, in most cases, to nearly solar values for the abundances, suggesting that the low abundances obtained from the ASCA data are probably artificial. Likewise, uncertainties in the plasma emissivity codes are critical and do not allow firm results concerning possible differences in the abundances.

As a general conclusion, our results show the presence of a very soft component and regions with temperatures well above 10^7 K in TTS, placing therefore strong constraints on models of the structure of the outer regions in these stars in terms of the temperature and density.

Another point worth raising is the use of the ratio L_X/L_{bol} as indicator of coronal activity since both L_X and L_{bol} scale in the same way with distance. For the stars in our sample these values are given in Table 7. The value for V410 Tau and TW Hya is near the empirical "saturation" level of about -3.0 (e.g. Fleming et al. 1995). This value is thought to represent the maximum efficiency at which dynamo activity can convert the star's internal energy into coronal X-ray emission. The value obtained for TW Hya, which is a CTTS, is not in agreement with the conclusion, based on the average properties of a large sample of stars, that CTTS are less saturated as compared to WTTS (Neuhäuser et al. 1995). However, this is still a controversial issue, with some WTTS showing a still higher $\log(L_X/L_{bol})$ level, as high as $\approx$ -2.6 (Alcalá et al. 1997). Nevertheless, while for V410 Tau and TW Hya L_X represents about 0.1% of the total luminosity, it seems that the mechanism responsible for the X-ray output is less efficient for CS Cha.

Table 7. Comparison between L_{bol} and L_X.

Object	L_X (10^{30} erg s^{-1})	Log (L_X/L_{bol})
V410 Tau (20 August)	7.36±0.11	-3.0
TW Hya	1.15±0.03	-3.0
CS Cha	1.48±0.08	-3.5

4.3. Variability

X-ray variability and activity are characteristics of TTS (for example, Feigelson & DeCampli 1981; Feigelson et al. 1993; Carkner et al. 1996). Therefore we have searched the PSPC observations for variability, both short- and long-term, as permitted by the data. ROSAT is a low orbit satellite and therefore the data are in sections of about 2500 seconds, separated by longer intervals. To guarantee that the analysis is not affected by background fluctuations we have constructed for each source the background - subtracted light curves shown in Figs. 8 to 10. From the plots it is easily seen that the shape of the curves does not show great differences for the stars in the sample. We will discuss that in the next section.

4.3.1. Short-term variability

Since the arrival time of each detected photon is recorded during the observation, the Kolmogorov-Smirnov (K-S) test for constancy was performed on the data. This test measures the maximum deviation of the photon arrival times from a constant source model. All sources show a probability larger than 95% for variability when the test is performed on the sorted time event files (corresponding to timescales of a few seconds).

On time scales between those of the sorted event files and minutes, CS Cha is the only star of our sample that shows clear evidence of variability (probability of about 99% for variation) for 10 seconds binned data.

We have also analysed the data divided into 300 seconds bins to test for variability on time scales of a few minutes. According to the K-S test, none of the sources shows variability on this time scale which is typical of flares. Therefore we conclude that no large flaring activity was present during the period of observations.

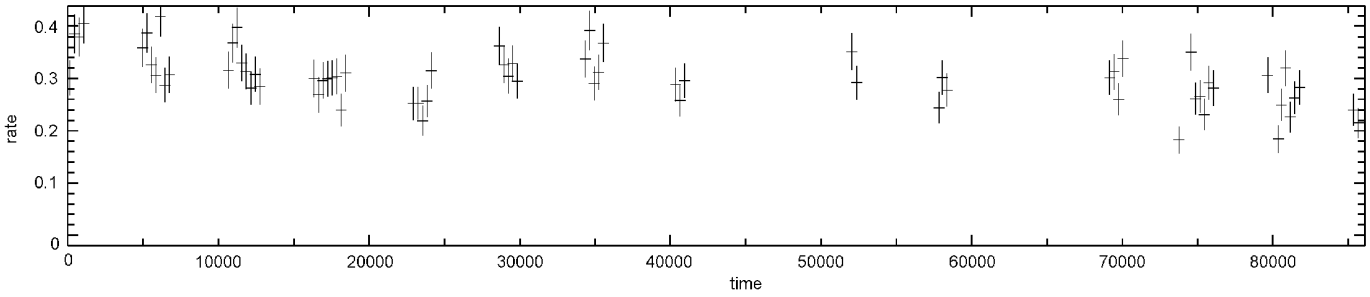

Fig. 8. Background-subtracted light curve for V410 Tau (20 August 1991) using 300 s bins. The plot shows the time in seconds from the beginning of the observation against count rate.

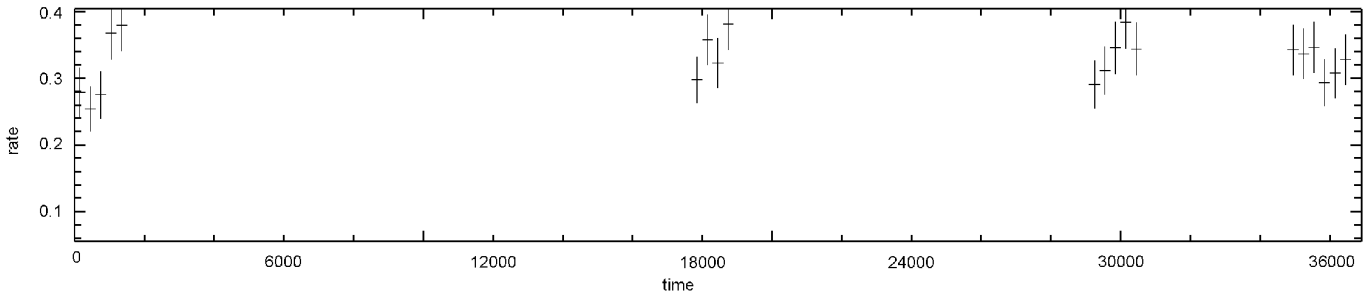

Fig. 9. As in Fig. 8 for TW Hya.

For V410 Tau, Strom & Strom (1994) also do not find any indication of flaring activity for the second period of observation (starting on 20 August 1991). However, their results indicating large amplitude variations in this star (for that same epoch) cannot be confirmed on time scales of minutes.

Although a visual inspection of the light curves (Figs. 8 to 10) suggests some variation on time scales of approximately 1200 seconds the K-S test does not confirm variability for the data divided in such bins.

Individual orbits can also provide time bins for tests of variability on a time scale of hours. The V410 Tau run starting on 20 August has sufficient 2500 seconds bins for a reliable analysis. The K-S test results are consistent with a source of constant flux (probability $>$99% for constancy), even though a gradually decreasing flux level seems apparent in Fig. 8. We have equally found no evidence for variations with the 1.87 day period reported for the optical data and interpreted as rotational modulation due to the presence of large surface spots (Sect. 2.2). The long exposure for CS Cha is also suitable for such an analysis. Once again the K-S test gives results compatible with a constant source. A close analysis of the light curve (Fig. 10) shows a variation in the count rate around $4.5\,10^5$ seconds which was however not confirmed by the K-S test.

4.3.2. Long-term variability

We have taken advantage of the separation between the pointing observations of V410 Tau to try and explore the variability on larger time scales, of months to years.

From Fig. 11 one can see that long-term variability is present in terms of count rate. There is a clear decrease in the count rate from March–August 1991 to September 1992, returning to high levels as shown by the HRI observation in February 1996. The HRI count rate has been converted to PSPC count rate using the HEASARC Pimms facility and adopting N_H = 2.66 and kT = 1.40. As for the variability on time scales of days, the four pointed observations taken in September 1993 only suggest a slight variation during such a period, given the error bars. In order to assure that the overall variations are in fact present and not only a result of large off-axis angles, Fig. 11 (bottom) also shows the count rate for some other sources close to V410 Tau in the same PSPC observation. The different light curves of these comparison stars (some of which in the 1991 exposures remain constant) allow us to conclude that V410 Tau is intrinsically variable.

For the PSPC observations, the spectral analysis shows that there is no significant variation in the values of the temperature of the cooler and hotter components for the different epochs. From the first to the second pointing, an increase in L_X is accompanied by an increase of the same order in the EM from the higher energy component, while the EM from the lower energy component does not exhibit significant variation. These variations imply that the amount of heated material has changed. However, it is difficult to address the question what this variation means in terms of the structure of the emitting region. The 2T model is not incompatible with the hypothesis that the X-ray emission is the result of plasma magnetically confined in coronal loops (Ciaravella et al. 1997). The details of such structures and their relation to a two-temperature model are still under discussion. Whatever the structure may be, these results indicate a change in the volume of the region responsible for the observed X-ray emission on a time scale of months to years.

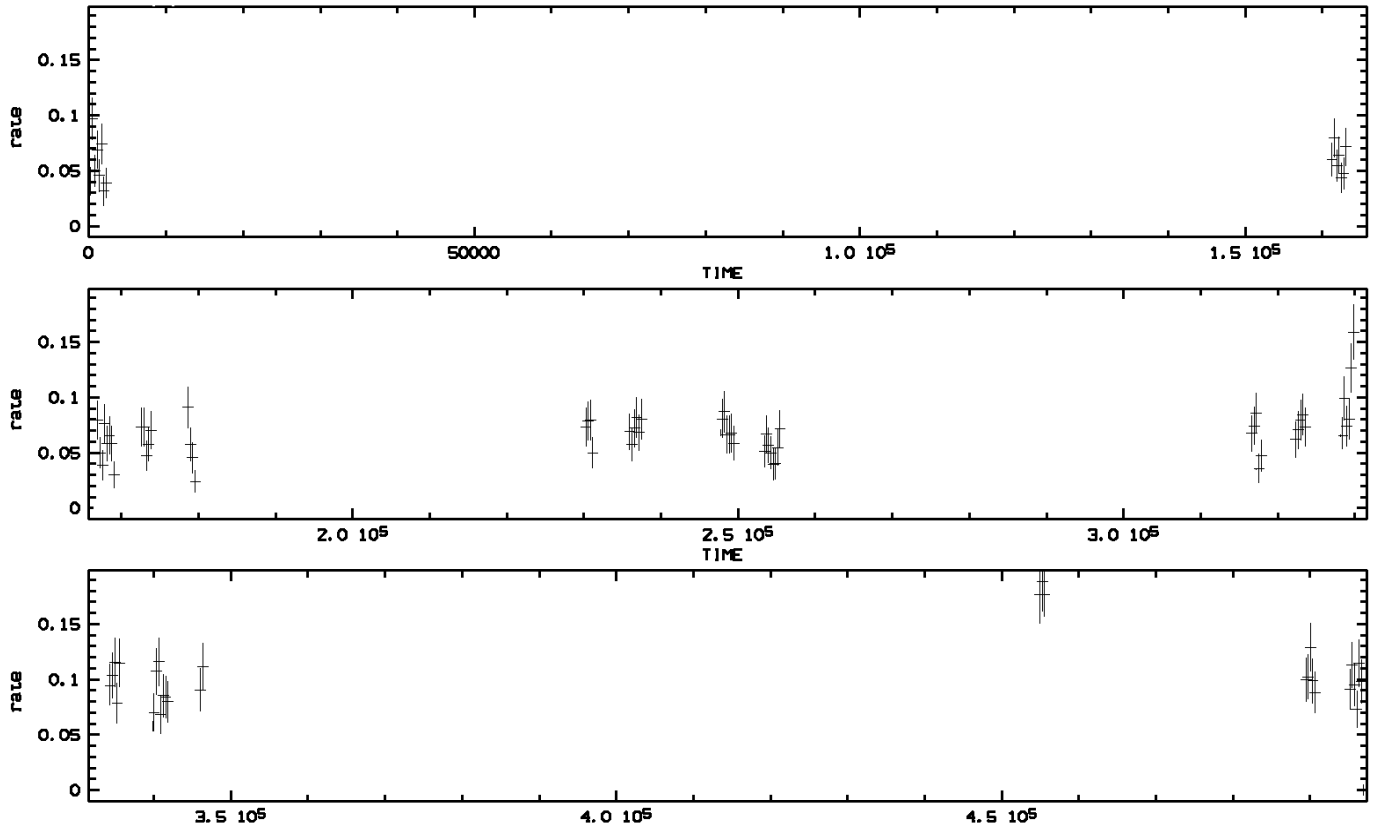

Fig. 10. As in Fig. 9 for CS Cha (18 February 1991).

5. Comparison with the Sun

The UV data analysis performed for several TTS has firmly established not only that TTS have line-emitting regions with temperatures up to 10^5 K but also that the emission from these regions is strongly enhanced relatively to the Sun. The surface fluxes are 10^3 to 10^4 times higher in TTS than in the Sun. Moreover, the distribution of material at the various temperatures is different from the Sun but also differs between the TTS themselves (Lago et al. 1984). We will next consider a similar analysis for our stars. We will add to the range of temperatures characteristic of the UV bands of IUE and associated flux levels for these three stars the values corresponding to still higher temperature regions using the X-ray data obtained with ROSAT (Sect. 4).

The UV emission lines may be interpreted as the result of purely thermal processes, i.e., of collisional excitation of the species present in collisional ionization equilibrium; thus to each emission process corresponds a peak temperature for that type of emission. In Fig. 12 we plot the ratio of stellar to solar fluxes for TW Hya, CS Cha and V410 Tau as a function of the peak temperature. The transitions occurring in the shorter UV band (1200 - 2000 Å) correspond to excitation temperatures between 10^4 - 10^5 K while temperatures of 10^7 K are representative of the ROSAT spectral band ($\approx$ 5 - 62 Å). This plot allows a direct comparison between the stellar and the solar emission line fluxes over that range of temperatures. The values for CS Cha and V410 Tau must be taken with some caution because the spectra are quite noisy. For comparison we also show the data points corresponding to two other well studied TTS: GW Ori and RU Lup, adapted from Lago et al. (1984).

As mentioned previously a major source of uncertainty is the value adopted for the radius of the stars. In any case, as Fig. 12 is concerned, an uncertainty of a factor of 2 in the radius will translate to a factor of 0.5 in the $\log(f_\star/f_\odot)$. Moreover, the uncertainties associated with the optical extinction cannot be neglected in this analysis. Taking for instance the unfavourable case of TW Hya, A_V in the range 0.10 - 0.25 will translate to an uncertainty in the surface flux of a factor of about 1.4. However, the overall shape of the curves will not be affected.

The X-ray points for the TTS in our sample correspond to values from ROSAT, whenever possible. For RU Lup we used a value corresponding to a ROSAT PSPC detection (Costa et al., in preparation). A similar value was found by Krautter et al. (1997). For the (non-flaring) solar X-ray luminosity within the ROSAT 0.2 - 2.4 keV band we have used $\sim 10^{27}$ erg s^{-1} (Güdel et al. 1997; see also Schmitt 1997). However, it is well known that the solar coronal output exhibits variations up to one order of magnitude. Therefore this value is taken as an "averaged quiet Sun". For the *Einstein* data point for GW Ori (0.5 - 4 keV energy band), the adopted X-ray luminosity for the Sun is 10^{26} erg s^{-1}, the same as used by Lago et al. (1984). We must point out that the X-ray flux for RU Lupi was obtained assuming a single temperature Raymond-Smith model (see Sect. 4) with kT = 1 keV due to the low number of counts. However, some more information about its emission can be gathered from the

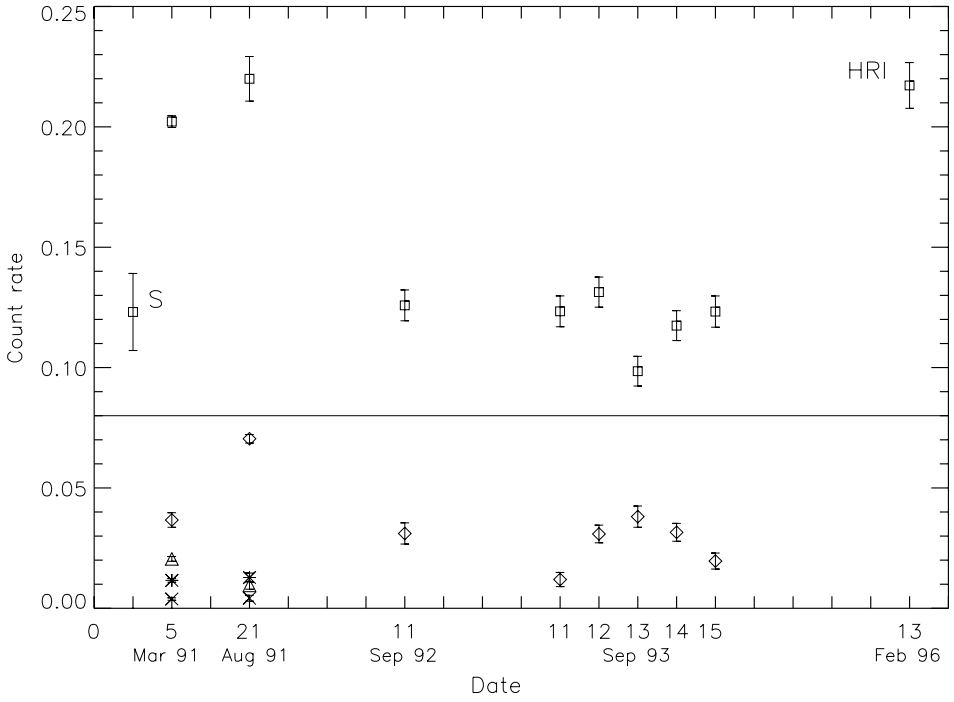

Fig. 11. Count rates for V410 Tau at different epochs (open squares). The first observation (S) is part of the ROSAT All-Sky Survey (Neuhäuser et al. 1995) and the 1996 observation (HRI) was taken with the High Resolution Imager. The lower plot shows the results for some comparison stars in the PSPC frames (see text for details). The diamonds correspond to a star present in all frames while other symbols represent the values for stars detected only in the better centred 1991 exposures.

hardness ratios (e.g. Alcalá et al. 1997). This analysis suggests that, unlike other CTTS (e.g. Neuhäuser et al. 1995), hard X-ray emission is not dominant in this star (Costa et al., in preparation). Therefore, the adopted X-ray flux is only an upper limit for the emission at temperatures of 10^7 K and probably most of the emission results from plasma at lower temperature.

As just indicated, the association of the X-ray data point with emission from plasma at 10^7 K needs some caution. In fact, lower temperature plasmas, down to 10^6 K, may also contribute to the flux. By separating both components responsible for the observed X-ray emission, we estimate the contribution of the lower temperature plasma to be roughly of the order of 30% for V410 Tau and CS Cha, even higher (around 40%) for TW Hya. However, these values should be taken only as indicative because the emission is more complex than just the pure addition of the fluxes emitted by the plasmas at the fitted temperatures.

Fig. 12 suggests that the energy output for TTS peaks at temperatures characteristic of the solar transition region. For RU Lupi, for example, this peak is followed by a clear and steep decrease in the emission at coronal temperatures. To a lesser extent this is also the behaviour for TW Hya and CS Cha. Yet for GW Ori and probably V410 Tau, the emission keeps on rising up to coronal temperatures. In any case the emission line fluxes at the various temperatures, from the chromosphere through the transition region up to the corona are always well above the solar values by one to four orders of magnitude. Note that the He II emission appears enhanced relative to the general trend for all stars that show significant X-ray emission. This raises the possibility of photoexcitation/photoionisation of He II by coronal X-rays. Such a scenario was proposed by Laming & Feldman (1993) in their analysis of solar prominence observations. Wahlstrom & Carlsson (1994) showed, again in the solar

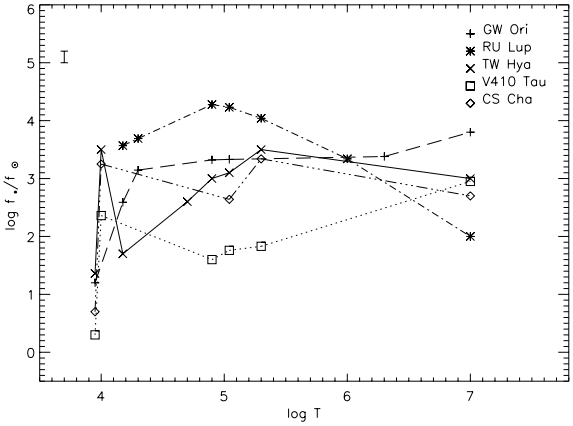

Fig. 12. Ratio of stellar to solar surface fluxes for TTS as a function of temperature. The figure shows that the distribution of material with temperature is in these stars different from that in the Sun. Furthermore it also shows that there are some differences among the TTS themselves. For V410 Tau the X-ray flux is an average ROSAT observations. A typical error bar is shown in the upper left corner. Due to the noisier spectra, for some lines in the spectra of V410 Tau and CS Cha the errors may be 50% higher than the error bar.

case, that the lines are formed, by cascade recombination from the n = 3 levels, following photoionisation from the ground state. We intend to examine the He II formation in T Tauri stars in detail in a separate work.

Furthermore, the plot shows differences in the structure of the atmosphere between these TTS. This might result from different exciting mechanisms operating in these stars. Namely, enhanced solar-like magnetic activity, variable magnetically driven winds, accretion or some combination of these. How-

ever, the picture is still far from clear and the identification of the mechanism(s) operating in any given star remains controversial. The discussion of this point is out of the scope of the present paper.

6. Conclusions

We have analysed newly calibrated IUE spectra and ROSAT data for three T Tauri stars: TW Hya, V410 Tau and CS Cha. These stars display different properties in terms of their optical spectra and have therefore been classified differently. While TW Hya has been classified as a CTTS and V410 Tau as a WTTS, CS Cha appears to be intermediate between these two classes.

In terms of the ultraviolet emission, the continuum seems in all three cases to be well explained by the sum of the stellar black body emission plus a hydrogenic component with a temperature in the range 1.4 to $5\,10^4$ K. Except for TW Hya, which requires a third component, namely black body emission at 7900 K covering approximately 5% of the stellar surface. This component is not referred to in the literature and may be due to a hot spot resulting from accretion, or some alternative form of magnetic activity. These are phenomena frequently proposed as explanations for the strong activity observed in this class of stars.

From the fitting of the ultraviolet continuum we are also able to infer a value for the interstellar extinction affecting each star.

In the ultraviolet spectra we have identified spectral lines formed in regions at temperatures up to 10^5 K and analysed the corresponding fluxes. In this respect, the behaviour of the three stars shows noticeable differences. While TW Hya and CS Cha display comparable levels of surface flux in the various lines, V410 Tau has a much lower level of emission for the higher excitation lines, namely N V, C IV and Si IV (more than one order of magnitude below). These stars have in common that they show emission strongly enhanced relatively to the Sun especially at the temperatures characteristic of the transition region. For TW Hya and CS Cha the excess surface fluxes relatively to the Sun reach factors exceeding 10^3.

Furthermore, we have established the connection from the UV to the X-ray band. This is important since it corresponds to extending the analysis from regions with plasma at temperatures below 10^4 K to regions at $\simeq 10^7$ K. Our results show that the behaviour of the three stars relatively to the Sun seems to extend in a harmonic way into the X-ray band.

The results of the X-ray spectral analysis for the three stars can be successfully described with a model of emission from two-temperature hot, optically thin plasma in collisional equilibrium, thus, confirming the thermal nature of the X-ray emission. The lowest temperature plasma is at about 10^6 K while the highest reaches 10^7 K. For the star V410 Tau the amount of material at those temperatures (as given by the emission measure) is systematically higher by a factor of 3 or even larger than that at characteristic UV temperatures (between $\simeq 10^4$ and a few 10^5 K).

We have also checked and found no evidence for strong flaring activity in our sources, at the time of the X-ray observations. Nevertheless, some level of variability is present for the stars in the sample at timescales of a few seconds. CS Cha is the only statistically confirmed variable source at slightly larger timescales (10 seconds). For V410 Tau the ROSAT observations show variations in terms of the observed count rate in time scales of months to years.

This work, making the connection between the ultraviolet and X-ray data for three TTS, allows a better understanding of the general properties of the structure of the atmosphere of the stars in the class. It constitutes an unreplaceable complement to other studies of activity in TTS we are carrying out in the optical, namely time-series analysis of high resolution line profiles. A detailed model of the atmospheric structure of some TTS using differential emission measure techniques is also being persued. Our 2T model is a very simple one, but the modest spectral resolution of the X-ray data does not justify the use of a more elaborate model. However, we stress that following the success of the fits to these low resolution spectra the detailed examination of individual lines could reveal important deviations from the assumed model. High resolution spectra from instruments with better capabilities such as those to be flown on board XMM and AXAF, hold a clear promise to improve our understanding of the high energy phenomena observed in this class of young and so extremely active stars.

Acknowledgements. We would like to thank the referee, Dr. Ralph Neuhäuser, for his helpful comments that improved the content of the paper. VMC wishes to thank the staff of Dunsink Observatory for his stay there while gaining experience in ROSAT data analysis and also acknowledges the grant PRODEP/96 - Acção 5.2 Medida 5. This work was partially supported by the Portuguese Fundação para a Ciência e Tecnologia through grants PESO/P/PRO/1196/97 and PESO/P/INF/1197/97. LN was supported by a TMR Fellowship.

References

Alcalá J.M., Krautter J., Schmitt J.H.M.M., et al., 1995, A&AS 114, 109
Alcalá J.M., Krautter J., Covino E., et al., 1997, A&A 319, 184
Basri G., Batalha C., 1990, ApJ 363, 654
Beckwith S., Sargent A., Chini R.S., Herbst T., 1990, AJ 99, 924
Bertout C., Basri G., Bouvier J., 1988, ApJ 330, 350
Bessel M.S., Brett J.M., 1988, PASP 100, 1134
Blondel P.F.C., Talavera A., Tjin A Djie H.R.E., 1993, A&A 268, 624
Bouvier J., 1990, AJ 99, 946
Bouvier J., Bertout C., Benz W., Mayor M., 1986, A&A 165, 110
Bouvier J., Bertout C., Bouchet P., 1989, A&AS 75, 1
Brooks D.H., Costa V.M., Lago M.T.V.T., Lanzafame A.C., 1999, MNRAS 307, 895
Cameron A.C., Campbell C.G., 1993, A&A 274, 309
Carkner L., Feigelson E.D., Koyama K., Montmerle T., Reid I.N., 1996, ApJ 464, 268
Casanova S., Montmerle T., Feigelson E.D., André P., 1995, ApJ 439, 752
Castro A.I.G., Fernández M., 1996, MNRAS 283, 55
Catala C., Bertout C., 1990, In: Rolfe E.J. (ed.) Evolution in Astrophysics: IUE Astronomy in the Era of New Space Missions. ESA SP-310, p. 11
Ciaravella A., Maggio A., Peres G., 1997, A&A 320, 945

Cohen M., Kuhi L.V., 1979, ApJS 41, 743
Costa V.M., Gameiro J.F., Lago M.T.V.T., 1999, MNRAS 307, L23
Cruddace R.G., Hasinger G.R., Schmitt J.H.M.M., 1988, In: Murtagh F., Heck A. (eds.) Astronomy from Large Databases. ESO Conference and Workshop Proceedings, p. 177
Edwards S., Cabrit S., Strom S.E., et al., 1987, ApJ 321, 473
Favata F., Maggio A., Peres G., Sciortino S., 1997, A&A 326, 1013
Feigelson E.D., DeCampli W.M., 1981, ApJ 243, 89
Feigelson E.D, Kriss G.A., 1989, ApJ 38, 262
Feigelson E.D., Casanova S., Montmerle T., Guibert J., 1993, ApJ 416, 623
Feigelson E.D., Welty A.D., Imhoff C., et al., 1994, ApJ 432, 373
Fernández M., Eiroa C., 1996, A&A 310, 143
Fernández M., Miranda L.F., 1998, A&A 332, 629
Fleming T.A., Schmitt J.H.M.M., Giampapa M.S., 1995, ApJ 450, 392
Gahm G.F., Fredga K., Liseau R., Dravins D., 1979, A&A 73, L4
Gahm G.F., Lodén K., Gullbring E., Harstein D., 1995, A&A 301, 89
Gauvin L.S., Strom K.M., 1992, ApJ 385, 217
Ghez A.M., Neugebauer G., Matthews K., 1993, AJ 106, 2005
Güdel M., Guinan E.F., Skinner S., 1997, ApJ 483, 947
Herbig G.H., Bell K.R., 1988, Lick Obs. Bull. 1111, 1
Herbst T.M., 1989, AJ 98, 2268
Herbst T.M., Koret D.L., 1988, AJ 96, 1949
Hoff W., Henning T., Pfau W., 1998, A&A 336, 242
Jensen E.L.N., Cohen D.H., Neuhäuser R., 1998, AJ 116, 414
Joncour I., Bertout C., Ménard F., 1994, A&A 285, L25
Kastner J.H., Zuckerman B., Weintraub D.A., Forveille T., 1997, Sci. 277, 67
Königl A., 1991, ApJ 370, L39
Krautter J., Wichmann R., Schmitt J.H.M.M., et al., 1997, A&AS 123, 329
Lago M.T.V.T., Gameiro J.F., 1998, MNRAS 294, 272
Lago M.T.V.T., Penston M.V., Johnstone R., 1984, In: Rolfe E.J., Battrick B. (eds.) Proc. of the Fourth European IUE Conference, ESA SP-218, p. 233
Laming J.M., Feldman U., 1993, ApJ 403, 434
Lawson W.A., Feigelson E.D., Huenemoerder D.P., 1996, MNRAS 280, 1071
Mewe R., Kaastra J.S., White S.M., Pallavicini R., 1996, A&A 315, 170
Montmerle T., Koch-Miramond L., Falgarone E., Grindlay J.E., 1983, ApJ 269, 182
Morrisson R., McCammon D., 1983, ApJ 270, 119
Neuhäuser R., Sterzik M.F., Schmitt J.H.M.M., Wichmann R., Krautter J., 1995, A&A 297, 391
Paresce F., 1984, AJ 89, 1022
Penston M.V., Lago M.T.V.T., 1983, MNRAS 202, 77
Petrov P.P., Scherbakov V.A., Berdyugina S.V., et al., 1994, A&AS 107, 9
Pfeffermann E., Briel U., Hippmann H., et al., 1986, In: Koch E.E., Schmahl G. (eds.) Proc. International Society for Optical Engineering, SPIE Vol. 773, p. 519
Preibisch T., 1997, A&A 320, 525
Preibisch T., Zinnecker H., Schmitt J.H.M.M., 1993, A&A 279, L33
Press W., Teukolsky S., Vetterling W., Flannery B., 1986, Numerical Recipes in FORTRAN. Cambridge University Press
Raymond J.C., Smith B.W., 1977, ApJS 35, 419
Reipurth B., Pedrosa A., Lago M.T.V.T., 1996, A&AS 120, 229
Rucinski S.M., Krautter J., 1983, A&A 121, 217
Savage B.D., Mathis J.S., 1979, ARA&A 17, 73
Schwartz R.D., 1992, In: Reipurth B. (ed.) Low Mass Star Formation in Southern Molecular Clouds. ESO, Garching, p. 93 (S92)
Schmitt J.H.M.M., 1997, A&A 318, 215
Schmitt J.H.M.M., Collura A., Sciortino S., et al., 1990, ApJ 365, 704
Schmitt J.H.M.M., Stern R.A., Drake J.J., Kürster M., 1996, ApJ 464, 898
Skinner S.L., Güdel M., Koyama K., Yamauchi S., 1997, ApJ 486, 886
Strom K.M., Strom S., 1994, ApJ 424, 237
Trümper J., 1983, Adv. Space Res. 2, 241
Uchida Y., Shibata K., 1984, PASJ 36, 105
Vrba F.J., Rydgren A.E., Chugainov P.F., Shakovskaia N.I., Zak D.S., 1986, ApJ 306, 199
Wahlstrom C., Carlsson M., 1994, ApJ 433, 417
Walter F.M., Kuhi L.V., 1981, ApJ 250, 254
Wichmann R., Krautter J., Covino E., et al., 1997, A&A 320, 185
Zimmermann U., Boese G., Becker T., et al., 1997, EXSAS User's Guide (MPE Report). Max-Planck-Institut für Extraterrestrische Physik